Thermal dependency of shell growth, microstructure, and stable isotopes in laboratory - reared Scapharca broughtonii (Mollusca: Bivalvia)

doi: 10.1002/2014GC005634

AGU PUBLICATIONS

Geochemistry, Geophysics, Geosystems

RESEARCH ARTICLE
10.1002/2014GC005634

Key Points:
- Thermal plasticity of shell microstructural formation was examined
- Relative volume of composite prismatic structure was greatest at cooler temperature
- Growth rates were correlated with volume of composite prismatic structure

Supporting Information:
- Supporting Information S1

Correspondence to:
K. Nishida,
koz-nishida@aist.go.jp

Citation:
Nishida, K., et al. (2015), Thermal dependency of shell growth, microstructure, and stable isotopes in laboratory-reared *Scapharca broughtonii* (Mollusca: Bivalvia), *Geochem. Geophys. Geosyst.*, *16*, 2395–2408, doi:10.1002/2014GC005634.

Received 24 OCT 2014
Accepted 26 JUN 2015
Accepted article online 2 JUL 2015
Published online 26 JUL 2015

Thermal dependency of shell growth, microstructure, and stable isotopes in laboratory-reared *Scapharca broughtonii* (Mollusca: Bivalvia)

Kozue Nishida[1,2], Atsushi Suzuki[1], Ryosuke Isono[3], Masahiro Hayashi[4], Yusuke Watanabe[4], Yuzo Yamamoto[4], Takahiro Irie[5], Yukihiro Nojiri[6], Chiharu Mori[5], Mizuho Sato[1,7], Kei Sato[8,9], and Takenori Sasaki[2]

[1]National Institute of Advanced Industrial Science and Technology, Geological Survey of Japan, Tsukuba, Japan, [2]The University Museum, University of Tokyo, Tokyo, Japan, [3]Marine Ecology Research Institute, Tokyo, Japan, [4]The Demonstration Laboratory, Marine Ecology Research Institute, Kashiwazaki, Japan, [5]Atmosphere and Ocean Research Institute, University of Tokyo, Kashiwa, Japan, [6]Center for Global Environmental Research, National Institute for Environmental Studies, Tsukuba, Japan, [7]Now at Asahi Geo-Survey Co. Ltd, Tokyo, Japan, [8]Department of Earth and Planetary Science, University of Tokyo, Tokyo, Japan, [9]Now at The University Museum, University of Tokyo, Tokyo, Japan

Abstract We experimentally examined the growth, microstructure, and chemistry of shells of the bloody clam, *Scapharca broughtonii* (Mollusca: Bivalvia), reared at five temperatures (13, 17, 21, 25, and 29°C) with a constant pCO_2 condition (~450 μatm). In this species, the exterior side of the shell is characterized by a composite prismatic structure; on the interior side, it has a crossed lamellar structure on the interior surface. We previously found a negative correlation between temperature and the relative thickness of the composite prismatic structure in field-collected specimens. In the reared specimens, the relationship curve between temperature and the growth increment of the composite prismatic structure was humped shaped, with a maximum at 17°C, which was compatible with the results obtained in the field-collected specimens. In contrast, the thickness of the crossed lamellar structure was constant over the temperature range tested. These results suggest that the composite prismatic structure principally accounts for the thermal dependency of shell growth, and this inference was supported by the finding that shell growth rates were significantly correlated with the thickness of the composite prismatic structure. We also found a negative relationship between the rearing temperature and $\delta^{18}O$ of the shell margin, in close quantitative agreement with previous reports. The findings presented here will contribute to the improved age determination of fossil and recent clams based on seasonal microstructural records.

1. Introduction

Molluscan shells are composed of calcium carbonate and exhibit a great variety of shell microstructures. These microstructures are classified according to criteria such as the orientation and aggregation of crystallites, the size and shape of crystallites or their structural units, the constituent minerals, and the presence or absence of an organic matrix [e.g., *Carter et al*., 1990]. Shell microstructures in Bivalvia have been studied predominantly in relation to taxonomy [*Taylor*, 1963; *Kobayashi*, 1971; *Uozumi and Suzuki*, 1981; *Carter*, 1990; *Sato et al*., 2013], phylogeny [*Taylor et al*., 1969, 1973; *Shimamoto*, 1986; *Hikida*, 1996], and crystallography [*Ubukata*, 2000; *Checa and Rodríguez-Navarro*, 2001; *Ubukata*, 2001a,b; *Checa et al*., 2009, 2013]. These studies have shown that some bivalve species crystallize shells with a single constituent mineral whereas others form a shell composed of both calcite and aragonite (e.g., a calcitic outer prismatic layer and an aragonitic inner nacreous layer in pearl mussels). Moreover, the shell microstructures made by a single individual can differ, depending on the environmental conditions it experiences during biomineralization [*Carter*, 1980]. For example, cyclical changes in the shell microstructure within a single shell layer have been observed in various taxa of Bivalvia [*Nishida et al*., 2011].

In family Arcidae, cyclical microstructural changes have been reported in both modern and fossil specimens (genera *Scapharca* and *Anadara*) [*Kobayashi and Kamiya*, 1968; *Kobayashi*, 1976a,b; *Nishida et al*., 2012]. *Nishida et al*. [2012] reported that the cyclical changes in the shell microstructures of *S. broughtonii* observed in field studies reflect seasonal temperature changes. These changes include variations in the relative

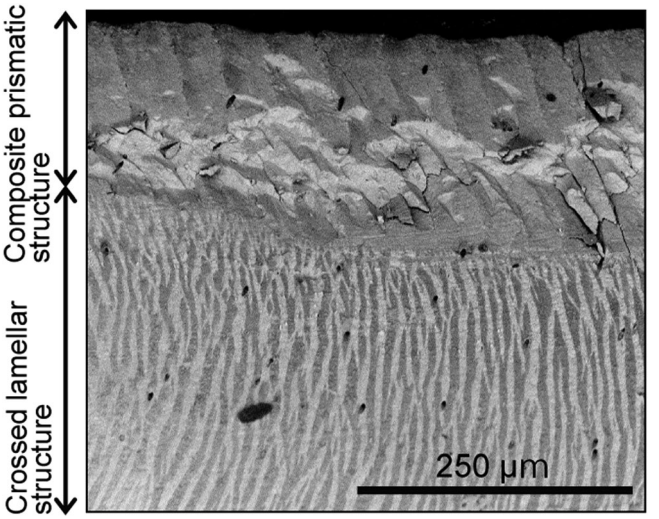

Figure 1. SEM photograph of a radial section of a specimen reared at 17°C. We define the outer layer as the structure outside the pallial myostracum. The outer shell layer is characterized by a composite prismatic structure on the exterior side of the shell and a crossed lamellar structure on the interior side.

thicknesses of composite prismatic and crossed lamellar structures in the outer layer (Figures 1 and 2). The relative thickness of the composite prismatic structure in the outer layer is greater in shell formed at cooler temperatures, whereas the crossed lamellar structure is relatively thicker in shell formed in summer. This relationship between temperature and microstructure can provide insight into biomineralization processes, and it also may be useful in paleoecological studies.

In this study, we focused on modern shell microstructures with the aim of applying the findings to fossil specimens. Methods for reconstructing paleoecological conditions from fossil specimens based on their skeletal microstructures may have an advantage over geochemical analyses of fossil shells, depending on the preservation state of the shells. The geochemical characteristics of calcareous fossils are often altered by recrystallization, cementation, or replacement of the materials in the original skeleton, and such contamination compromises paleotemperature estimates based on geochemical proxies [*Ragland et al*., 1979; *Popp et al*., 1986; *Elorza and García-Garmilla*, 1998]. On the other hand, many studies have demonstrated that skeletal microstructures can be identified not only in specimens that include partly recrystallized, cemented, or replaced materials [*Rush and Chafetz*, 1990; *Elorza and García-Garmilla*, 1998] but also from shell molds [*Kouchinsky*, 2000; *Vendrasco et al*., 2010]. Hopefully, observation of seasonality in shell microstructures will expand our ability of accurate age determination in fossil specimens.

It is well known that the isotopic composition of biominerals depends on the environmental conditions when and where calcification occurred. For example, shell $\delta^{18}O$, which reflects both the temperature and the oxygen isotope composition of the seawater where the biomineralization occurred, is commonly used to reconstruct seawater temperatures in the field [*Watanabe and Oba*, 1999; *Nakashima et al*., 2004; *Watanabe et al*., 2004; *Chauvaud et al*., 2005; *Owen et al*., 2008]. However, accumulating evidence from corals suggests that skeletal growth rates also affect isotope ratios through a kinetic isotope effect. This effect is caused by isotopic disequilibria (reactions with molecules with heavier isotopes are slower), and if not accounted for properly, it creates a serious bias in the estimation of environmental parameters. *McConnaughey and Gillikin* [2008] hypothesized that in molluscs, relatively mild alkalinization and the use of catalysis by carbonic anhydrase at the calcification site suppress the kinetic isotope effect, by reducing the contribution of CO_2 hydroxylation to isotopic disequilibrium [see also *Owen et al*., 2002, 2008].

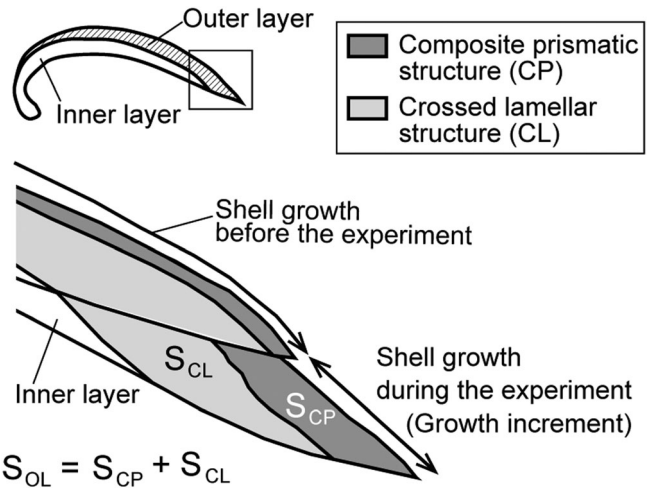

Figure 2. Schematic diagram of the measurement areas on an acetate peel from a shell section. S_{OL}, S_{CL}, and S_{CP} are the area of the outer layer, the crossed lamellar structure, and the composite prismatic structure, respectively; S_{OL} is equal to the sum of S_{CL} and S_{CP}.

In this study, we reared mud-dwelling bivalves at five temperatures to

examine the thermal plasticity of shell microstructural formation and shell growth strategies. We selected the bloody clam, *Scapharca broughtonii* (subfamily Anadarinae), as a research target because recent and fossil specimens of subfamily Anadarinae (Mollusca: Bivalvia: Arcidae) show cyclicity of shell microstructures [*Kobayashi* and *Kamiya*, 1968; *Kobayashi*, 1976a,b; *Nishida et al*., 2012] and the fossil record of this subfamily extends back to the Oligocene [*Noda*, 1966; *Eames*, 1967; *Noda*, 1986]. *Scapharca broughtonii* is distributed in the sea of Japan, the East China Sea, the northwest Pacific, and the northern Philippine Sea [*Habe*, 1965; *Evseev and Lutaenko*, 1998; *Matsukuma and Okutani*, 2000]. We evaluated the relationship between water temperature and shell microstructural formation to gain insight into the biomineralization process. In addition, we examined the stable carbon and oxygen isotopes of the aragonite shells of these bivalves with the aim of improving techniques for extracting information about environmental conditions during calcification of both fossil and recent shell specimens. Finally, on the basis of our results, we discuss the possible adaptive significance of the thermal dependency of skeletal growth and microstructure formation in *S. broughtonii*.

2. Materials and Methods

2.1. Sample Collection and Experimental Design

Living *S. broughtonii* collected on 27 June 2012 were provided by the Kudamatsu Institute of Mariculture in Kudamatsu City, Yamaguchi Prefecture, and immediately transported to the Demonstration Laboratory, Marine Ecology Research Institute, in Kashiwazaki City, Niigata Prefecture, Japan, for our experiments. No individuals died during the transfer. All specimens were 1 year old juveniles, which are suitable for observing growth, in contrast to sexually matured individuals (2–4 years old) growing very slowly [*Sasaki*, 1997; *Minobe*, 2007]. Prior to the experiment, the individuals were kept in tanks at approximately 23°C for approximately 2 months to allow the juvenile clams to acclimatize to the new environment. During this period, we provided phytoplankton as food twice a day via a siphon (inside diameter, 0.8 mm); each feeding consisted of a mixture of equal volumes of *Pavlova lutheri* (3–5 $\times$ 10^6 cells mL^{-1}) and *Tetraselmis tetrathela* (1–2 $\times$ 10^6 cells mL^{-1}).

We built a flowthrough experimental tank system for the present study (Figure 3). The individuals were randomly assigned to five 12 L transparent plastic tanks (the experimental tanks, external size: length 37 cm, width 22 cm, height 25 cm, flow rate 1 L min^{-1}, open to the atmosphere) so that each tank contains 5–7 experimental individuals. Beginning on 28 August 2012, we changed the temperature of the water in the experimental tanks in a stepwise manner (by 1°C each day from 23°C) until temperatures reached the target values of 13, 17, 21, 25, and 29°C. During the experimental period, the actual temperatures in experimental tanks, which were recorded every 10 min by digital data loggers (Figure 4), were 13.2 $\pm$ 0.5, 17.2 $\pm$ 0.4, 20.9 $\pm$ 0.3, 24.7 $\pm$ 0.3, and 28.5 $\pm$ 0.3°C (mean $\pm$ SD, Table 1). During the experiment, 600 mL of the phytoplankton mixture described above was added to each tank twice a day via a siphon. We stopped the seawater flow for 2 h during teach feeding. Because each experimental tank was placed in a 53 L polypropylene tank (the outer tank, external size: 57 cm $\times$ 38 cm $\times$ 30 cm deep) filled with overflow or bypass seawater of the experimental tank (Figure 1), the change in water temperature in the experimental tanks during the feeding time was minimal.

Temperature, partial pressure of carbon dioxide (pCO_2), dissolved inorganic carbon (DIC), aragonite saturation state (Ω_{arag}), and pH in the experimental tanks are shown in Table 1. Both experimental [*Millero*, 1995] and observational [*Weiss et al*., 1982] evidence indicates that pCO_2 in seawater depends positively on temperature all other conditions being equal. In addition, seawater pCO_2 level varies with the atmospheric CO_2 concentration; as a result of air-sea gas exchange, the seawater tends to converge to equilibrium with the overlying atmosphere. Therefore, in an open system, colder seawater has greater DIC and lower Ω_{arag}. From these principles, it follows that in a closed system with artificially cooled seawater, pCO_2 decreases. This effect transiently prevents reproducing the pCO_2 condition of the surface ocean in laboratory, because the surface seawater (regarded as an open system) is expected to have an approximately constant pCO_2 during all seasons, being in equilibrium with the atmosphere. To avoid this problem and to establish *natural* rearing conditions in the experiment, we controlled the chemical status of the seawater as follows.

First, we installed four 500 L tanks in which sand-filtered, thermoregulated seawater (at 13, 17, 25, and 31°C) was continuously supplied at flow rate of $\sim$1 L min^{-1} from the chiller/heater unit of the laboratory (Figure 3).

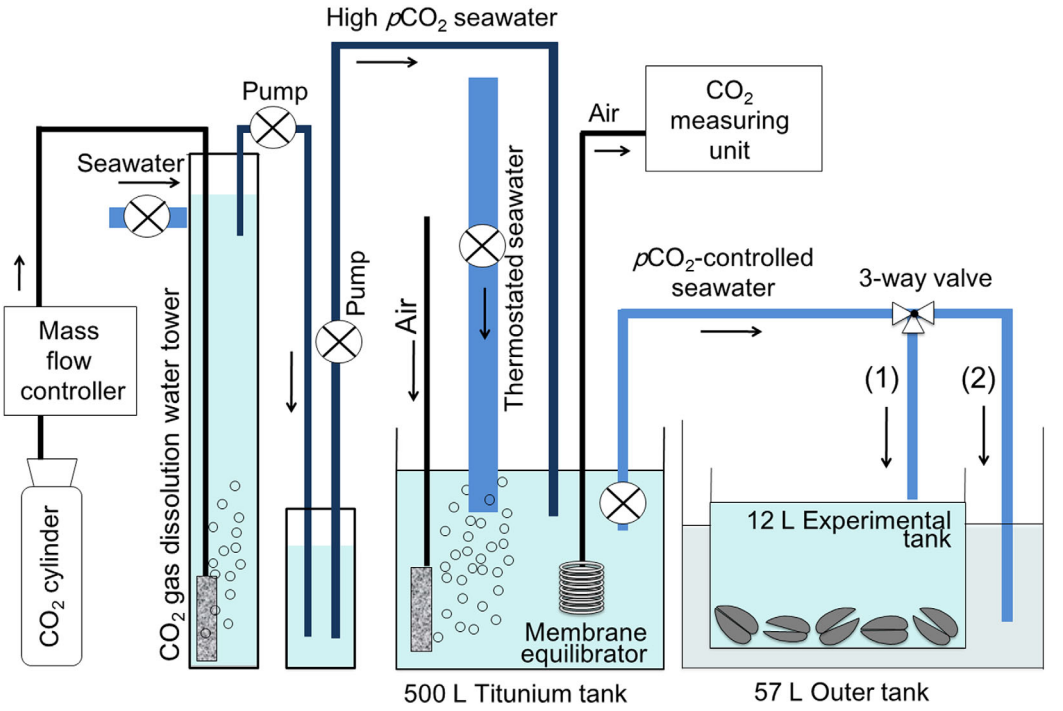

Figure 3. The schematic diagram of culturing tank system used in the study. Temperature-regulated and pCO_2-ajdusted seawater was usually supplied to the experimental tank and overflow seawater was filled in the outer tank (route 1). During the feeding time, seawater supply to the experimental tanks stopped for 2 h and bypass seawater was supplied directly to the outer tank (route 2). See the text for detailed explanation.

These 500 L tanks were intensively aerated to get the seawater pCO_2 equilibrated to the atmospheric level. We also installed a closed tower (1.9 m in height; head space: 0.2 m) to prepare high pCO_2 seawater (~17,000 μatm) by bubbling carbon dioxide gas from a compressed CO_2 gas cylinder. The high pCO_2 seawater was then continuously added to the 500 L tanks with a tube pump to compensate the pCO_2 drop caused by the artificial temperature control. Seawater in the 21°C treatment was made up by mixing seawater from the 17°C and 25°C tanks, and fine thermal adjustment was achieved by a chiller/heater unit (Earth Co., Ltd.). Finally, the seawater was supplied to the 12 L experimental tanks, so that pCO_2 was maintained at approximately 450 μatm across all treatments (Table 1).

The temperature and CO_2 concentration of the seawater in the five experimental tanks were monitored at 2 h intervals throughout the experiment with a nondispersive infrared analyzer system (Model SCD-12, Kimoto Electric Co. Ltd.). Water samples were collected twice a week from the tubes connecting the 500 and 12 L tanks, and total alkalinity and salinity were measured with a total alkalinity analyzer (Model ATT-05, Kimoto Electric Co. Ltd.) and an inductive salinometer (Watanabe Keiki MFG. Co., Ltd), respectively. The seawater pH, DIC, and Ω_{arag} were calculated from the measured pCO_2 and the total alkalinity, temperature, and salinity by using the computer program CO2CALC [*Robbins et al*., 2010] (http://cdiac.ornl.gov/oceans/CO2SYS_calc_MAC_WIN.html). In this calculation, we used the apparent dissociation constants for carbonic acid originally proposed by *Mehrbach et al*. [1973], and then refit by *Dickson and Millero* [1987]. The saturation state of seawater with respect to aragonite, Ω_{arag}, is the product of the concentrations of the calcium and carbonate ions ($[Ca^{2+}]$, $[CO_3^{2-}]$), divided by the stoichiometric solubility product (K^*_{sp}):

$$\Omega_{arag} = [Ca^{2+}][CO_3^{2-}]/K^*_{sp}$$

The carbon dioxide concentration in seawater ($[CO_2(aq)^*]$) increased and the carbonate ion concentration ($[CO_3^{2-}]$) decreased as temperature decreased across the tanks (Table 1) [*Orr et al*., 2005; *Fabry et al*., 2008]. The actual Ω_{arag} in the lowest temperature tank (1.81) was within the range of the winter Ω_{arag} value 2010 in *S. broughtonii* habitats, as estimated by *Yara et al*. [2012] ($1.0 < \Omega_{arag} < 2.7$). Thus, the addition of CO_2 to the low-temperature tanks seemed to successfully mimic the habitat environment of this species with respect to Ω_{arag} values.

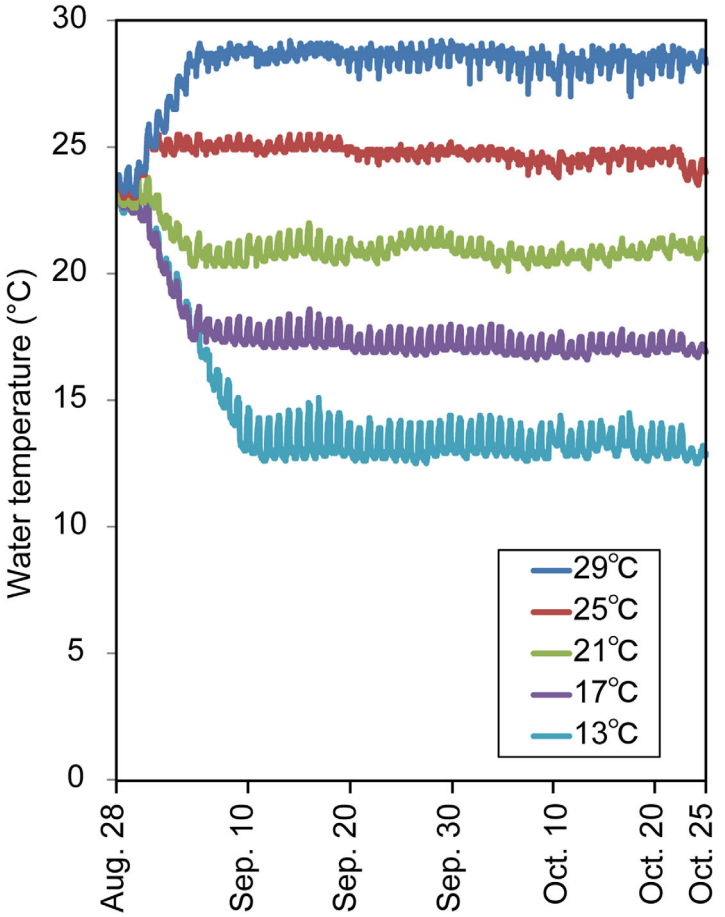

Figure 4. Water temperature in each 12 L experimental tank during the rearing experiment. To reduce the potential for physiological stress caused by the temperature change, the temperature settings were increased or decreased from 23°C in daily increments of 1°C beginning on 28 August 2012 and ending when the target experimental temperature was reached.

2.2. Measurement of Shell Sizes

Prior to the experiment, the periostracum covering the external margin of the shells was partly removed to create a marker for identifying subsequent shell growth (Figure 5a); once a part of the shell is bared, it is never recovered by periostracum, but newly constructed shell is covered. Growth was quantified by measuring shell height on 22 and 24 October 2012 (just before the experiment and near the end of the

Table 1. Temperature, pCO_2, DIC, pH, $[HCO_3^-]$, $[CO_3^{2-}]$, and the Saturation State of Seawater With Respect to Aragonite at the In Situ Temperature (Ω_{arag}) for Each Treatment[a]

Treatment	Temperature (°C) Mean ±1 SD	Maximum	Minimum	pCO_2 (μatm)	DIC* (μmol/kgSW)	$[HCO_3^-]$* (μmol/kgSW)	$[CO_3^{2-}]$* (μmol/kgSW)	pH*	Ω_{arag}*
13°C	13.2 ± 0.5	15.1	12.5	450 ± 12	1999	1864	117	7.982	1.81
17°C	17.2 ± 0.4	18.6	16.6	451 ± 14	1974	1823	134	7.984	2.10
21°C	20.9 ± 0.3	22.0	20.1	450 ± 14**	1948	1782	151	7.986	2.39
25°C	24.7 ± 0.3	25.5	23.5	450 ± 16	1921	1739	169	7.986	2.72
29°C	28.5 ± 0.3	29.2	27.0	450 ± 15	1893	1693	188	7.984	3.09

[a]Water samples were collected from water supply tubes to 12 L experimental tanks, through which pCO_2-controlled water was supplied from 500 L tanks, and the arithmetic means of salinity and total alkalinity (TA) over the experimental period were 32.4 ± 0.2 and 2156 ± 16 μmol kg^{-1}, respectively (mean, 1 SD). While pCO_2 in the 500 L mixing tanks of 13, 17, 25, 29°C was measured values, that of 21°C was the average pCO_2 value of 17 and 25°C (**). For temperatures, the average and standard deviation of all data, together with mean daily maximum and minimum values in each experimental tank are shown. The pH (total hydrogen ion scale), DIC, $[HCO_3^{2-}]$, $[CO_3^{2-}]$, and Ω_{arag} were calculated from the observed and analytical values using CO2CALC software [*Robbins et al*., 2010], the temperature and salinity given in this table, and the apparent dissociation constants for carbonic acid of *Mehrbach et al*. [1973], refit by *Dickson and Millero* [1987]. Units of concentration are μmol kg^{-1} and those of pCO_2 are μatm. An asterisk (*) indicates calculated value by CO2CALC software.

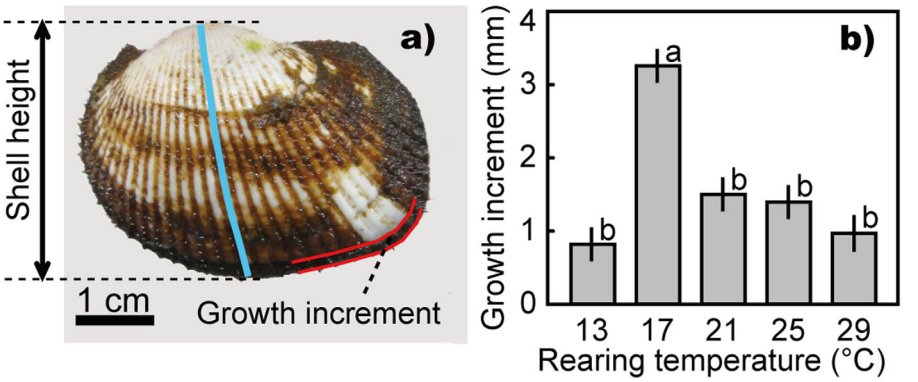

Figure 5. Biometry of the experimental specimens ($N = 34$). (a) A photograph of an experimental specimen. Prior to the experiment, the periostracum covering the external margin of the shell was partly removed to create a marker for identifying subsequent shell growth. After the periostracum removal, periostracum is newly secreted from the mantle in parallel with the formation of new shell. The red lines show the shell growth increment, and the blue line indicates where the shell was sectioned for the acetate peel respectively. (b) Mean growth increment normalized by the initial shell height (covariate) and the standard error of individuals reared at five temperatures. Different letters on the bars indicate a statistically significant difference between treatments (ANCOVA followed by the Tukey-Kramer HSD test, $\alpha = 0.05$).

experiment, respectively). We measured each individual three times with electronic calipers (instrumental error, $\pm$0.02 mm), and then calculated the arithmetic mean (Table S1). The directly measured distance between the shell margin at the beginning and that at the end of the experiment was used as the measure of the shell growth increment in the statistical analysis, in which the null hypothesis was that the growth increment did not differ across treatments. To test the hypothesis, the shell growth increment was analyzed by applying a general linear model with temperature as a fixed-effect factor and shell height at the beginning of the experiment as a covariate. We used the Shapiro-Wilk test to confirm the residual normality ($W = 0.95$; $p = 0.13$) and the Bartlett test to confirm homoscedasticity among treatments ($p = 0.08$), and we used the Tukey-Kramer HSD test for post hoc multiple comparisons on the covariate-adjusted dependent variable ($\alpha = 0.05$). We used JMP statistical software (SAS Institute Inc.) for all statistical analyses.

2.3. Scanning Electron Microscopy Observations of Shell Microstructures

The microstructures of 15 randomly selected specimens were observed by the acetate peel method [*Kennish et al*., 1980] and by scanning electron microscopy (SEM). In other words, one valve of each specimen was radially sectioned along a radial rib oriented perpendicular to the hinge line (Figure 5a), and then etched with 0.2% acetic acid for 5–10 min. In this paper, we use "composite prismatic structure" and "crossed lamellar structure" as defined by *Carter et al*. [1990] to describe shell microstructures. The thickness and cross-sectional areas of the composite prismatic structure and the entire outer layer were measured by using ImageJ/NIH version 1.45 image analysis software (http://imagej.nih.gov/ij/) (Figure 2). The thickness of the composite prismatic structure was measured as the perpendicular distance from the inner edge of the structure to the outer shell surface, and the thickness of the outer layer was measured as the distance between the inner and outer shell surfaces. The cross-sectional area of each structure was measured within the growth increment (Figure 2). We normalized the area of the composite prismatic structure by that of the outer layer (S_{CP}/S_{OL}) to cancel the effect of size variation among individuals.

2.4. Stable Isotope Analysis of Shell and Seawater

We sampled small aliquots of shell carbonate from the external margin of the outer layer (distance from the margin, 0.0–0.5 mm) of 17 specimens using a dental drill. These samples, each weighing approximately 70–110 μg, were reacted with 104% H_3PO_4 at 25°C in a custom-made carbonate preparation device [*Ishimura et al*., 2004], and the isotopic ratios were determined with a Micromass Isoprime mass spectrometer. We report the oxygen and carbon isotope ratios of the shells ($\delta^{18}O_c$ and $\delta^{13}C_c$) relative to Vienna Peedee Belemnite (V-PDB), adopting the consensus values of $-2.20‰$ and $1.95‰$ for $\delta^{18}O_c$ and $\delta^{13}C_c$, respectively, of the NBS 19 international reference standard relative to V-PDB. The precision was $<0.10‰$ and $<0.05‰$ (1 SD) for $\delta^{18}O$ and $\delta^{13}C$, respectively, of the shell samples. We collected a seawater sample from each rearing tank for seawater $\delta^{18}O$ measurement ($\delta^{18}O_w$) on 11 September, and for $\delta^{13}C$ of DIC in seawater ($\delta^{13}C_{DIC}$) on 21 October. The isotopic values of the seawater samples were measured with a Thermo-Fisher Scientific

Table 2. Average Annual Seawater Temperatures and Their Ranges at the Seven Main *S. broughtonii* Fisheries Around Japan[a]

Main Fishing Ports of *S. broughtonii* Around Japan	Depth (m)	Temperature Range (°C)	Average (°C)	SD
Mutsu Bay, Aomori Prefecture, Japan	20	7.9–22.0	15.1	5.4
	30	7.8–21.0	14.5	5.1
Off the coast of Miyagi Prefecture, Japan	20	8.7–21.0	14.3	4.7
	30	8.7–19.5	13.7	4.4
Tokyo Bay, Tokyo, Japan	20	13.9–23.0	18.0	3.5
	30	14.3–21.9	17.7	3.1
Nanao Bay, Ishikawa Prefecture, Japan	20	9.9–25.1	16.8	5.3
	30	9.9–24.2	16.3	5.1
Mikawa Bay, Aichi Prefecture, Japan	20	14.7–24.2	19.2	3.7
	30	15.0–22.6	18.7	3.2
Seto Island Sea, Yamaguchi Prefecture, Japan	20	10.1–24.2	17.1	4.9
	30	10.6–23.8	17.3	4.8
Ohmura Bay, Nagasaki Prefecture, Japan	20	15.5–26.1	20.4	3.8
	30	15.4–25.6	20.1	3.6

[a]The temperature data are from the Japan Oceanographic Data Center (JODC, http://www.data.jma.go.jp/obd/stats/etrn/index.php). The average habitat depth of *S. broughtonii* is 20–30 m. The average annual seawater temperature at the seven main *S. broughtonii* fisheries in Japan approximately ranges from 14.3 to 20.4°C (20 m depth) and from 13.7 to 20.1°C (30 m).

DELTA plus XL mass spectrometer at SI Science Co., Japan. The precision was $<0.05‰$ and $<0.10‰$ (1 SD) for $\delta^{18}O_w$ and $\delta^{13}C_{DIC}$, respectively. All $\delta^{18}O_w$ values are reported relative to Vienna Standard Mean Ocean Water (V-SMOW) and $\delta\ ^{13}C_{DIC}$ values are reported relative to V-PDB. Because $\delta^{18}O$ of shell carbonate is affected by both water temperature and $\delta^{18}O$ of the ambient seawater, to remove the effect of $\delta^{18}O_w$ on the $\delta^{18}O$ of the shell carbonate, we subtracted $\delta^{18}O_w$ from the shell carbonate $\delta^{18}O$.

2.5. Analyses of Total Inorganic and Organic Carbon

To quantify the amount of organic matrix in the shell microstructures, the organic matter content of an adult specimen collected from Tachibana Bay, Nagasaki Prefecture, was measured by General Environmental Technos Co., Ltd. (KANSO Technos). We collected powdered samples of the composite prismatic and crossed lamellar structures from a single valve of this specimen, after visually identifying the two microstructures on an acetate peel made from a radial section of the specimen to avoid cross contamination between them. First, the total carbon (TC) content of approximately 3–5 mg of powdered sample was measured with a CHN analyzer (2400CHN II, PerkinElmer) with a flame temperature of 1030°C. Next, the total inorganic carbon (TIC) content of 10–30 mg of powdered sample was determined with a coulometer (CM5011, UIC). The total organic carbon (TOC) content was then calculated by subtracting TIC from TC (TOC = TC – TIC). Both TC and TIC were measured in triplicate, and the resulting precision was <0.12% (1 SD) and 0.35% (1 SD), respectively. The propagated error of TOC was <0.37% (1 SD).

3. Results and Discussion

3.1. Shell Growth of *S. broughtonii* at Five Temperatures

Analysis of covariance results indicated that rearing temperature significantly affected the shell growth increment ($p < 0.05$). The effect of the initial shell height was not significant ($p > 0.05$), suggesting that the size variation before the experiment can be ignored when examining the observed relationship between temperature and shell growth. The subsequent post hoc test showed the growth increment at 17°C to be significantly greater than that in the other treatments (Figure 5b). This best-performance temperature is close to the average seawater temperature at the habitat depth of *S. broughtonii* (20–30 m), based on estimates obtained at the locality where the experimental individuals were sampled (Yamaguchi Prefecture; see Table 2). The relationship curve between temperature and somatic growth rates is commonly hump shaped in ectotherms [*Angilletta*, 2009].

$\delta^{13}C_c$ ranged from $-1.09‰$ to $-0.48‰$, and $\delta^{18}O_c$ ranged from $-2.68‰$ to $+0.17‰$ (Table S2). The measured values of $\delta^{13}C_{DIC}$ and $\delta^{18}O_w$ were also shown in Table S2. The $\delta^{18}O_c - \delta^{18}O_w$ of the specimens cultured between 17 and 29°C was negatively correlated with water temperature ($R = 0.98$, $p < 0.01$; Figure 6a), suggesting that in *S. broughtonii*, shell $\delta^{18}O$ is a good indicator of temperature over this temperature range, as previously demonstrated by *Grossman and Ku* [1986]. Exceptionally, the specimens reared at 13°C obviously deviated from the linear relationship between seawater temperature and $\delta^{18}O$ (Figure 6a). This anomaly

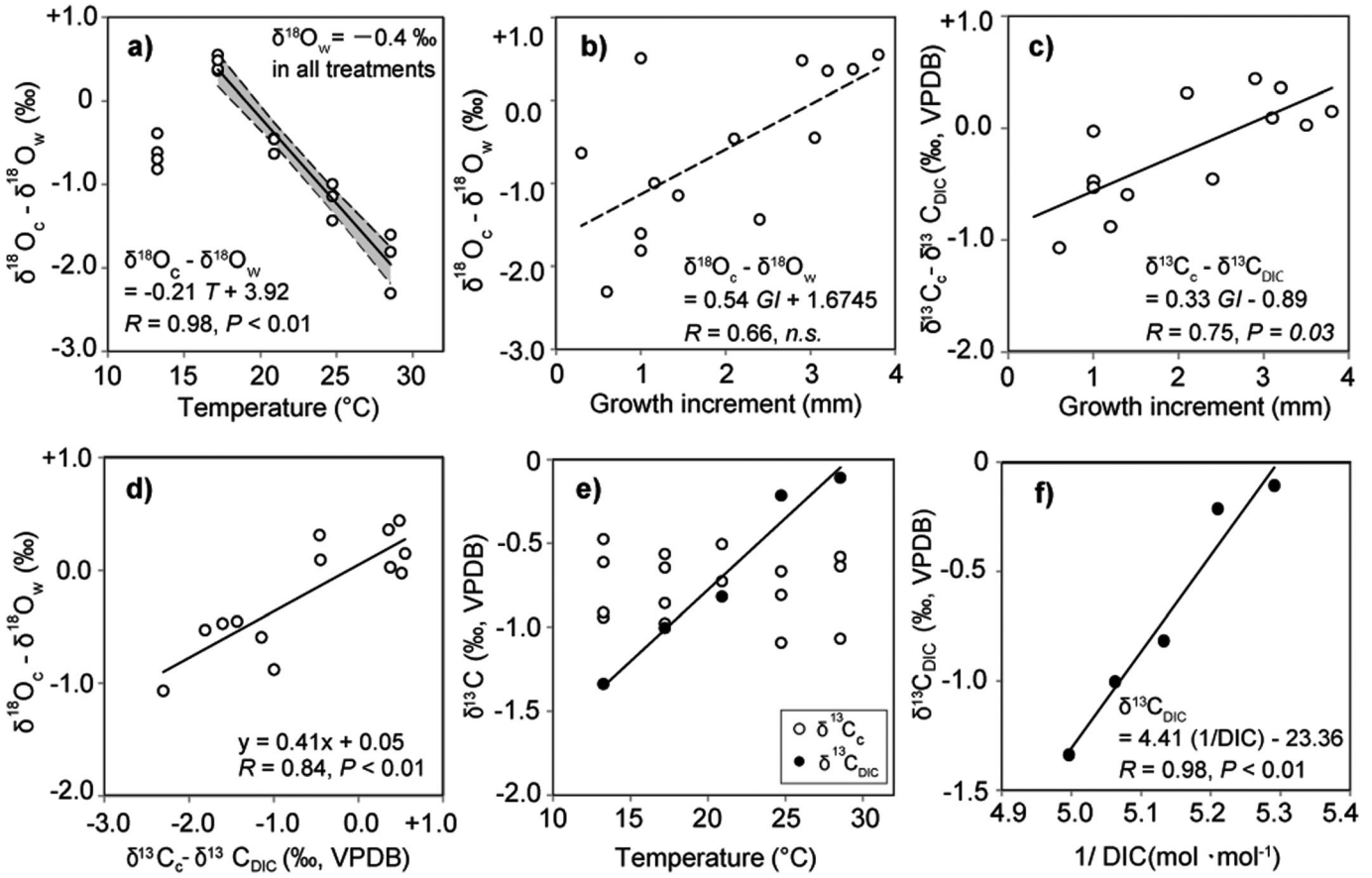

Figure 6. $\delta^{18}O$ and $\delta^{13}C$ values of 17 specimens reared at five different temperatures. (a) Relationship between the difference $\delta^{18}O_c - \delta^{18}O_w$ and water temperature. Mean ± 1 SD of $\delta^{18}O_w$ was −0.39‰ ± 0.01‰. The correlations between these two variables were strong at 17, 21, 25, and 29°C. $\delta^{18}O_c$ and $\delta^{18}O_w$ indicate $\delta^{18}O$ of shell carbonate and seawater, respectively. A regression line (with 95% confidence intervals) was fit to the data for 17–29°C. Relationships between (b) the difference $\delta^{18}O_c - \delta^{18}O_w$ and growth increment, (c) $\delta^{13}C_c - \delta^{13}C_{DIC}$ and growth increment, and (c) the difference $\delta^{18}O_c - \delta^{18}O_w$ and $\delta^{13}C_c - \delta^{13}C_{DIC}$ for 17–29°C, respectively. (e) $\delta^{13}C$ of shell carbonate ($\delta^{13}C_c$) and $\delta^{13}C$ of dissolved inorganic carbon (DIC) in seawater ($\delta^{13}C_{DIC}$) at the five temperatures. (f) Keeling plot showing the relationship between the $\delta^{13}C_{DIC}$ composition and the reciprocal of DIC at five temperatures. n.s., not significant.

was presumably caused by shell fragments of shell that were mineralized before the experiment (during the acclimatization period) becoming accidentally mixed in with the analyzed samples, because at 13°C shell growth was negligible and accurate microsampling was difficult.

Growth increment at 17–29°C was positively correlated with both $\delta^{18}O_c - \delta^{18}O_w$ ($R = 0.66$, $p > 0.05$) and $\delta^{13}C_c - \delta^{13}C_{DIC}$ ($R = 0.75$, $p = 0.03$) (Figures 6b and 6c). The correlation between $\delta^{18}O_c - \delta^{18}O_w$ and $\delta^{13}C_c - \delta^{13}C_{DIC}$ in the experimental specimens maintained at 17–29°C was positive ($R = 0.84$, $p < 0.01$; Figure 6d). *McConnaughey* [2003] hypothesized that the kinetic isotope effects are always accompanied by (1) the negative correlation between skeletal growth rate and oxygen and carbon isotope ratios and (2) the positive correlation between skeletal oxygen and carbon isotope ratios. The positive correlation observed between $\delta^{18}O_c - \delta^{18}O_w$ and $\delta^{13}C_c - \delta^{13}C_{DIC}$ of the present study might be an indication of kinetic isotope effects. But, correlations between growth increment and the oxygen and carbon isotope ratios of *S. broughtonii* specimens were both negative, suggesting the absence of kinetic isotope effects. *McConnaughey and Gillikin* [2008] hypothesized that the kinetic isotope effect is suppressed in molluscan shells because the contribution of CO_2 hydroxylation to isotopic disequilibria is reduced. Our finding of positive correlations between the growth rates and the skeletal isotopic compositions, opposite to the relationships in corals [*McConnaughey*, 2003], might support their hypothesis.

The significant positive correlation that we observed between the $\delta^{13}C_c - \delta^{13}C_{DIC}$ and shell growth (Figure 6c) might be attributable to changes in metabolic carbon availability. $\delta^{13}C$ of molluscan shell carbonate depends on both calcification physiology and environmental conditions (see *McConnaughey and Gillikin* [2008] for a

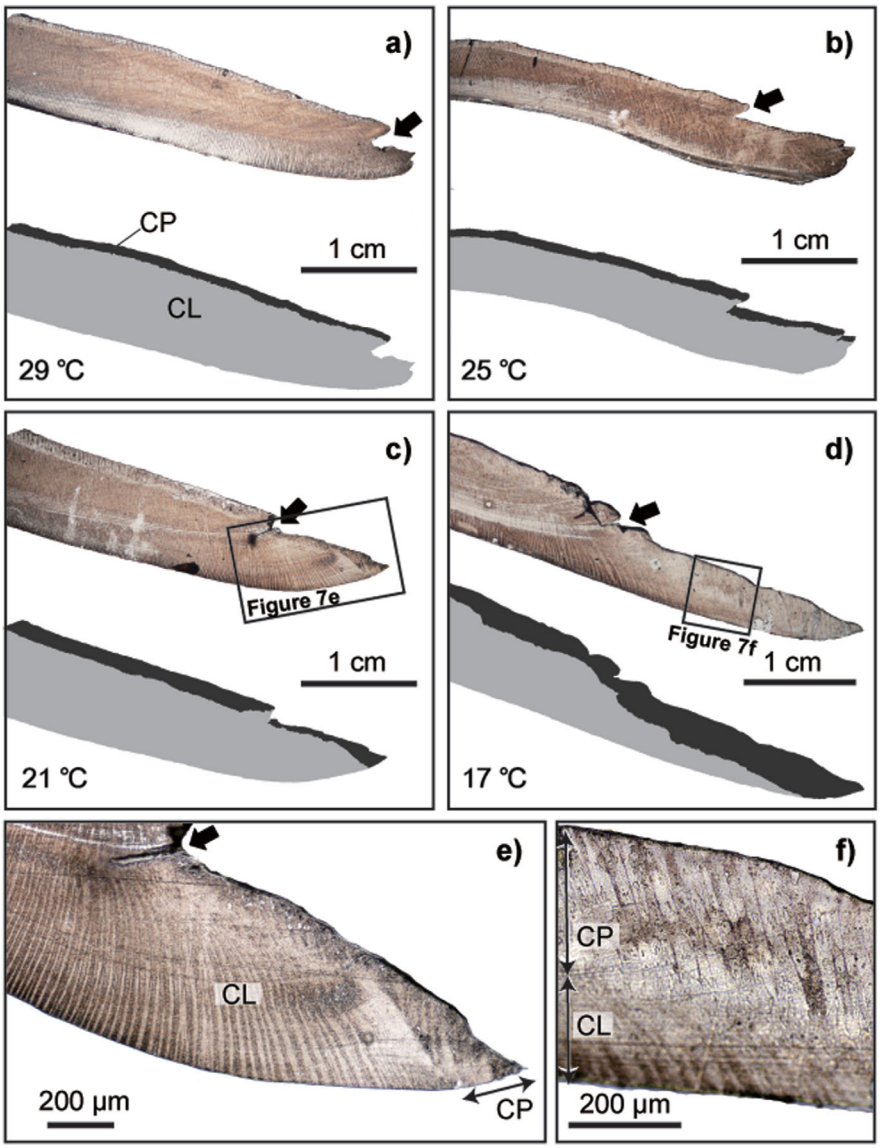

Figure 7. Photographs and sketches of acetate peels of radial sections of the shell margins of experimental specimens reared at (a) 29, (b) 25, (c) 21, and (d) 17°C. Arrows indicate the distinct notches resulting from growth breaks. Close-ups showing the microstructures in the growth increments of (e) c and (f) d. CP, composite prismatic structure; CL, crossed lamellar structure.

review). Among physiological processes, both aging [*Lorrain et al*., 2004; *Gillikin et al*., 2007] and shell growth rates [*Klein et al*., 1996; *Owen et al*., 2002] have been shown to affect shell $\delta^{13}C$. *Lorrain et al*. [2004] suggested that the ratio of respiratory CO_2 availability to the shell precipitation rate increases as the shell growth rates decrease during ontogeny. In our experiment, the *S. broughtonii* specimens were of the same age, but growth rates decreased at lower water temperatures, and $\delta^{13}C_c - \delta^{13}C_{DIC}$ was lower at the lower growth rates. Thus, in *S. broughtonii*, $\delta^{13}C$ might reflect a temperature-induced physiological effect, namely, an increasing contribution of metabolic carbon to shell calcification.

3.2. Microstructural Changes Observed at Different Temperatures

The shells of all specimens cultured at four temperatures (from 17°C to 29°C) exhibited distinct notches, indicating a growth break (a period of slow or stopped growth) (Figures 7a–7e). These growth breaks probably occurred when we transferred the specimens to the temperature-controlled experimental tanks and partly removed the periostracum. The presence of the growth break made it easy to identify the timing of the commencement of the experiment on the shell cross sections. The composite prismatic and crossed

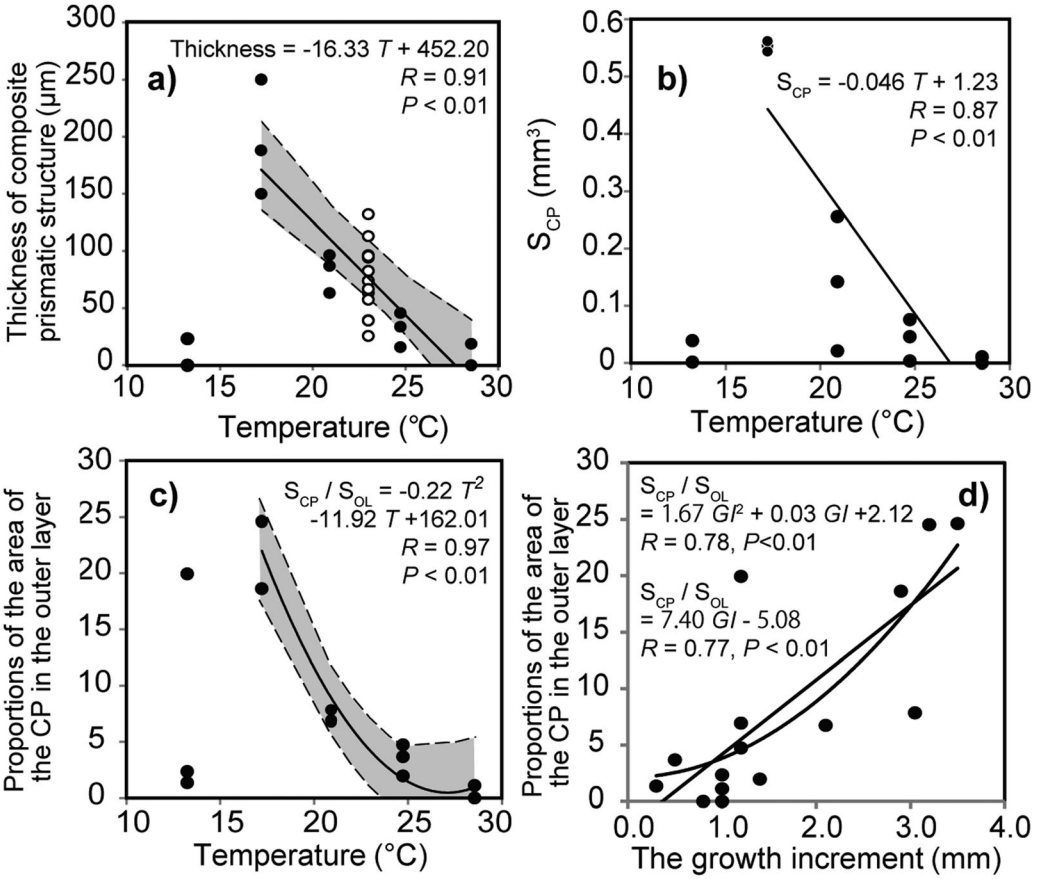

Figure 8. Relationships between thicknesses and areas of shell microstructures in radial sections, temperature, and growth rate in the experimental specimens. (a) Relationship between temperature and composite prismatic structure thickness; $N = 15$. Open circles indicate the composite prismatic structure thickness before the experiment, and close circles are the thickness at the end of the experiment; $N = 15$. A regression line (with 95% confidence intervals) was fit to the data for 17–29°C. (b) Relationship between water temperature and the area of composite prismatic structure (S_{CP}); $N = 15$. (c) Relationship between temperature and S_{CP}/S_{OL} (the relative area of the composite prismatic structure (CP) relative to the total outer layer area, S_{OL}). A quadratic curve (with 95% confidence intervals) was fit to the data for 17–29°C. (d) Relationship between S_{CP}/S_{OL} and the growth increment. A regression line and a quadratic curve were fit to the data for 17–29°C; $N = 12$.

lamellar structures in the outer layer could be clearly distinguished by SEM (Figure 2) and on the acetate peels (Figure 7). The thickness of the composite prismatic structure decreased as the temperature increased from 17°C to 29°C (Figure 8a); as this relationship was observed in field-collected specimens [*Nishida et al*., 2012].

From 17°C to 29°C, both S_{CP} and S_{CP}/S_{OL} showed significant negative correlations with water temperature (Figures 8b–8d), and S_{CP}/S_{OL} was positively correlated with the growth increment (Figure 8d). The latter relationship is noteworthy, because it suggests that winter shell growth mainly accounts for the increase in the area of the composite prismatic structure observed in the field [*Nishida et al*., 2012]. In the specimens cultured at 13°C, both S_{CP} and S_{CP}/S_{OL} were smaller and more variable than the same parameters at 17°C (Figures 8b and 8c). This might because no shell growth occurred at 13°C and these values reflect growth status at a temperature above 13°C during the 8 day temperature adjustment period at the beginning of the experiment (see Figure 4).

3.3. Thermal Dependency of Shell Microstructural Formation

We assumed the following linear relationship between water temperature (T°C) and aragonite-water fractionation:

$$\delta^{18}O_c - \delta^{18}O_w = aT + b,$$

where a and b are constants. From the ordinary regression analysis, the least squares estimates of a and b (and their standard errors) were −0.21 (±0.01) and 3.92 (±0.31) (see Figure 6a). The slope in *S. broughtonii*

Table 3. δ^{18}O-Temperature (T) Sensitivities of Inorganic and Biogenic Aragonite

Reference	δ^{18}O-T Sensitivity (‰/°C)	Source of Carbonate
This study	−0.21	Bivalve
Watanabe and Oba [1999]	−0.26	Bivalve
Grossman and Ku [1986]	−0.23	Mollusc and foraminifera
Böhm et al. [2000]	−0.20	Coralline sponge
Böhm et al. [2000]	−0.23	Coralline sponge, mollusc, and foraminifera
Gagan et al. [2012]	−0.08 to −0.22	Coral
Kim et al. [2007]	−0.21	Inorganic aragonite

(−0.21‰ °C^{-1}) is close to other published values for both biogenic [*Grossman and Ku*, 1986; *Watanabe and Oba*, 1999; *Böhm et al.*, 2000; *Gagan et al.*, 2012] and inorganic aragonite [*Kim et al.*, 2007] (Table 3).

Moreover, the thickness of the composite prismatic structure and the relative area of the composite prismatic structure in the outer layer also correlated negatively with water temperature (Figures 8a and 8c). The microstructures in the outer layer could be easily identified by SEM and by optical microscope observation of shell cross sections; therefore, it should be possible to use the relative area of the composite prismatic structure for age determination and paleotemperature estimation. In fact, *Sugiura et al.* [2014] proposed a good example, in which the pattern of microstructure thickness in the outer layer reflects the seasonal temperature fluctuation, and can be used for age determination in *S. broughtonii*.

In this study, shell δ^{13}C did not correlate significantly with water temperature and it varied independently of $\delta^{13}C_{DIC}$ (Figure 6e). $\delta^{13}C_{DIC}$ showed considerable variation among the five temperature regimes (Figure 6f). We attribute this variation to the addition of CO_2 gas to adjust pCO_2 and Ω_{arag} in each experimental tank. A keeling plot of the relationship between $\delta^{13}C_{DIC}$ and the reciprocal of DIC at the five temperatures (Figure 6f) clearly indicates that the addition of CO_2 gas led to the $\delta^{13}C_{DIC}$ gradient across the five experimental tanks. In some species of molluscs, shell δ^{13}C values are often close to $\delta^{13}C_{DIC}$ values (reviewed in *McConnaughey and Gillikin* [2008]), but this is not always the case. In some land snail taxa, carbon for shell building is derived from dietary organic matter (e.g., genus *Helix*) [see *Stott*, 2002], which is transferred to the extrapallial fluid through respiration, and thus affects δ^{13}C in the calcifying space. No significant correlation was observed between $\delta^{13}C_{DIC}$ and shell δ^{13}C, suggesting that the seawater DIC, which showing a δ^{13}C temperature gradient, contributes less to shell δ^{13}C in *S. broughtonii* than respiration-derived carbon.

3.4. The Link Between Shell Growth and Shell Microstructure Formation: A Possible Clue to Understanding Thermal Plasticity in Marine Calcifiers?

Analysis of TIC and TOC fractions (%) in three powdered microstructure samples (sample sizes; $N_{CP} = 3$ and $N_{CL} = 3$) from a single specimen of *S. broughtonii*, the TOC fraction (%, relative to total carbon) of the composite prismatic structure was higher than that of the crossed lamellar structure (Table 4), a result consistent with the findings of *Taylor and Layman* [1972], reporting that composite prismatic structure is richer in organics than crossed lamellar structure in bivalves. Although empirical evidence is not yet available, increasing the S_{CP}/S_{OL} ratio enable the increase in the rate of shell growth possible at lower temperatures, if protein synthesis is more easily achieved than calcification at low temperatures [see *Irie et al.*, 2013]. This conjecture is compatible with the observed increase in the S_{CP}/S_{OL} with decreasing temperature in *S. broughtonii* (Figure 8c). However, there seem an disadvantage in increasing the S_{CP}/S_{OL} ratio; *Taylor and Layman* [1972] and *Currey* [1976] demonstrated on the basis of compression strength data that the composite prismatic structure is physically weaker than the crossed lamellar structure in *Mercenaria mercenaria* (Bivalvia: Veneridae) [see also *Yang et al.*, 2011], although further study is required to determine whether this holds true in *S. broughtonii*. Therefore, the possibility that a trade-off exists between growth and physical factors (e.g., strength and elasticity) should be considered in investigations of thermal adaptation by bivalves, including *S. broughtonii*.

Table 4. Percentages of Total Carbon (TC), Total Inorganic Carbon (TIC), and Total Organic Carbon (TOC) in a Shell of *S. broughtonii*[a]

Microstructure	Total Carbon (%)	Total Inorganic Carbon (%)	Total Organic Carbon (%)
Composite prismatic structure	11.75	11.04	0.72
Crossed lamellar structure	11.69	11.51	0.19

[a]The powdered samples were microsampled from each microstructure in a single valve of an adult specimen.

The mechanisms of formation of shell microstructures in individuals have been studied in relation to crystallography [*Checa et al.*, 2009; *Checa et al.*, 2013], fracture

mechanics [*Meyers et al*., 2008; *Yang et al*., 2011], and molecular biology [*Zhang and Zhang*, 2006; *Marie et al*., 2012]. The expression of genes for shell layer-specific shell matrix proteins is known to differ in different areas of the mantle [e.g., *Marie et al*., 2012]. *Marie et al*. [2012] also suggested that different secretory repertoires control the biomineralization processes of prism and nacre deposition in the pearl oyster shell. However, little information is available on the mechanisms of plasticity of shell microstructural formation in a single shell layer. *Joubert et al*. [2014] examined expression of mantle genes for shell matrix proteins in the pearl oyster, *Pinctada margaritifera*, and pointed out that by measuring the expression of genes for shell matrix proteins, it is possible to evaluate biomineralization activity, such as shell growth rates at different temperatures and different microalgal concentrations (i.e., food availability). In the present study, *S. broughtonii* displayed not only qualitative but also quantitative changes in shell microstructure under different temperature conditions. Further studies from the perspective of crystallography, fracture mechanics, and molecular processes are needed to understand how varying environmental conditions affect microstructure formation and, thus, how molluscs cope with locally and globally heterogeneous environmental conditions.

Significant insight might be gained by considering our results in the broader context of thermal plasticity in calcifying ectotherms. Most ectotherms achieve a larger body size when growing at cooler temperatures compared with warmer temperatures [*Atkinson*, 1994, 1995; *Atkinson and Sibly*, 1997; *O'Dea and Okamura*, 2000]. This type of phenotypic plasticity is referred to as the temperature-size rule, and its significance has been examined from the viewpoint of adaptation. *Irie et al*. [2013] suggested that marine calcifiers might not comply with this rule, however, because the cost of slow shell growth in cold waters might outweigh the benefit of a larger soft body at lower temperatures. In fact, *Burton and Walter* [1987] have shown that the precipitation rate of inorganic aragonite and calcite in seawater is positively correlated with water temperature. In our experiment, however, we found the opposite patterns; that is, in *Scapharca broughtonii*, growth increment negatively depended on water temperature (except at 13°C) (Figure 5b). It is possible that most marine calcifiers do in fact follow the temperature-size rule [e.g., *Irie and Fischer*, 2009; *Chauvaud et al*., 2012], contrary to the hypothesis put forward by *Irie et al*. [2013].

4. Conclusion

We examined the thermal plasticity of shell microstructural formation in *S. broughtonii* by experimentally rearing premature individuals at five constant temperature regimes keeping seawater pCO_2 at ~450 μatm. The relative volume of composite prismatic structure in the outer layer was greatest at their optimal growth temperature (17°C), which was consistent with the trend observed in field-collected specimens. In the temperature range between 17 and 29°C, faster growth at lower temperatures is achieved by dominantly building the composite prismatic structure (with a greater S_{CP}/S_{OL} ratio), probably accompanied by the cost of increased physical vulnerability to durophagous predation. We also found a negative relationship between rearing temperature and $\delta^{18}O$ of shell margin ($-0.21‰$/°C), and thus $\delta^{18}O$ of the shell of *S. broughtonii* is useful as a paleothermometer. Our findings will contribute to the development of paleontological techniques based on fossil shell microstructure as well as provide a new insight to understanding evolutionary significance of calcification by marine calcifiers.

Acknowledgments

We thank Kazuyoshi Endo, Toshihiro Kogure, Takanobu Tsuihiji, Hodaka Kawahata, and paleontological seminar members of University of Tokyo for their suggestions on research methods and their comments; Toyoho Ishimura, Rei Nakashima, and Yumiko Yoshinaga at AIST for their suggestions on stable isotopic analysis and their comments; the members of MERI and Takeshi Yoshimura (The Central Research Institute of Electric Power Industry) for suggestions on culturing methods and comments; Yuji Kuyama, Makoto Fukui (Kudamatsu Institute of Mariculture, Kudamatsu, Japan), and the other members of this institute and Shizuka Murakami (Kudamatsu, Japan) for the donated specimens; and the members of ELSS Co. Ltd. for English editing. Nicola Allison and anonymous Reviewers provided helpful comments of our manuscript. This study was supported by The Environment Research and Technology Development Fund (A-1203), Mikimoto Fund for Marine Ecology, the Sasakawa Scientific Research grant from The Japan Science Society, and a grant from the Fujiwara Natural History Foundation. This study was also supported by KAKENHI 24244090, 26220102 funded by JSPS, and a research fund from AIST.

References

Angilletta, M. J. (2009), Temperature and the life history, in *Thermal Adaptation: A Theoretical and Empirical Synthesis*, edited by M. J. Angilletta, pp. 157–180, Oxford Univ. Press, N. Y.

Atkinson, D. (1994), Temperature and organism size—A biological law for ectotherms?, *Adv. Ecol. Res.*, *25*, 1–58, doi:10.1016/S0065-2504(08)60212-3.

Atkinson, D. (1995), Effects of temperature on the size of aquatic ectotherms: Exceptions to the general rule, *J. Therm. Biol.*, *20*(1), 61–74, doi:10.1016/0306-4565(94)00028-H.

Atkinson, D., and R. M. Sibly (1997), Why are organisms usually bigger in colder environments? Making sense of a life history puzzle, *Trends Ecol. Evol.*, *12*(6), 235–239, doi:10.1016/S0169-5347(97)01058-6.

Böhm, F., M. M. Joachimski, W. C. Dullo, A. Eisenhauer, H. Lehnert, J. Reitner, and G. Wörheide (2000), Oxygen isotope fractionation in marine aragonite of coralline sponges, *Geochim. Cosmochim. Acta.*, *64*(10), 1695–1703, doi:10.1016/S0016–7037(99)00408-1.

Burton, E. A., and L. M. Walter (1987), Relative precipitation rates of aragonite and Mg calcite from seawater: Temperature or carbonate ion control?, *Geology*, *15*, 111–114, doi:10.1130/0091-7613(1987)15<111:RPROAA>2.0.CO;2.

Carter, J. G. (1980), Environmental and biological controls of bivalve shell mineralogy and microstructure, in *Skeletal Growth of Aquatic Organisms: Biological Records of Environmental Change (Topics in Geobiology)*, edited by D. C. Rhoads and R. A. Lutz, pp. 69–113, Plenum, N. Y.

Carter, J. G. (1990), Evolutionary significance of shell microstructure in the Palaeotaxodonta, Pteriomorphia and Isofilibranchia (Bivalvia: Mollusca), in *Skeletal Biomineralization: Patterns, Processes and Evolutionary Trends*, vol. I, edited by J. G. Carter, pp. 135–296, Van Nostrand Reinhold, N. Y.

Carter, J. G., et al. (1990), Glossary of skeletal biomineralization, in *Skeletal Biomineralization: Patterns, Processes and Evolutionary Trends*, vol. I, edited by J. G. Carter, pp. 609–661, Van Nostrand Reinhold, N. Y.

Chauvaud, L., A. Lorrain, R. B. Dunbar, Y. M. Paulet, G. Thouzeau, F. Jean, G. Jean-Marc, and D. Mucciarone (2005), Shell of the Great Scallop *Pecten maximus* as a high-frequency archive of paleoenvironmental changes, *Geochem. Geophys. Geosyst.*, *6*, Q08001, doi:10.1029/2004GC000890.

Chauvaud, L., et al. (2012), Variation in size and growth of the great scallop *Pecten maximus* along a latitudinal gradient, *PloS one*, *7*(5), e37717, doi:10.1371/journal.pone.0037717.

Checa, A. G., and A. Rodríguez-Navarro (2001), Geometrical and crystallographic constraints determine the self-organization of shell microstructures in Unionidae (Bivalvia: Mollusca), *Proc. R. Soc. London, Ser. B*, *268*(1468), 771–778, doi:10.1098/rspb.2000.1415.

Checa, A. G., A. Sánchez-Navas, and A. Rodríguez-Navarro (2009), Crystal growth in the foliated aragonite of monoplacophorans (Mollusca), *Cryst. Growth Des.*, *9*, 4574–4580, doi:10.1021/cg9005949.

Checa, A. G., J. T. Bonarski, M. G. Willinger, M. Faryna, K. Berent, B. Kania, A. González-Segura, C. M. Pina, J. Pospiech, and A. Morawiec (2013), Crystallographic orientation inhomogeneity and crystal splitting in biogenic calcite, *J. R. Soc. Interface*, *10*, 20130425, doi:10.1098/rsif.2013.0425.

Currey, J. D. (1976), Further studies on the mechanical properties of mollusc shell material, *J. Zool.*, *180*, 445–453, doi:10.1111/j.1469-7998.1976.tb04690.x.

Dickson, A., and F. Millero (1987), A comparison of the equilibrium constants for the dissociation of carbonic acid in seawater media, *Deep Sea Res., Part A*, *34*, 1733–1743, doi:10.1016/0198-0149(87)90021-5.

Eames F. E. (1967), A new arcid species from Holland, *Proc. Malacol. Soc. London*, *34*, 299–302.

Elorza, J., and F. García-Garmilla (1998), Palaeoenvironmental implications and diagenesis of inoceramid shells (Bivalvia) in the mid-Maastrichtian beds of the Sopelana, Zumaya and Bidart sections (coast of the Bay of Biscay, Basque Country), *Palaeogeogr. Palaeoclimatol. Palaeoecol.*, *141*(3), 303–328, doi:10.1016/S0031-0182(98)00058-3.

Evseev, G. A., and K. A. Lutaenko (1998), Bivalves of the subfamily Anadarinae (Arcidae) from Vietnam, *Malacol. Rev.*, *7*, suppl. I, 1–37.

Fabry, V. J., B. A. Seibel, R. A. Feely, and J. C. Orr (2008), Impacts of ocean acidification on marine fauna and ecosystem processes, *ICES J. Mar. Sci.*, *65*(3), 414–432, doi:10.1093/icesjms/fsn048.

Gagan, M. K., G. B. Dunbar, and A. Suzuki (2012), The effect of skeletal mass accumulation in *Porites* on coral Sr/Ca and δ^{18}O paleothermometry, *Paleoceanography*, *27*, PA1203, doi:10.1029/2011PA002215.

Gillikin, D. P., A. Lorrain, L. Meng, and F. Dehairs (2007), A large metabolic carbon contribution to the δ^{13}C record in marine aragonitic bivalve shells, *Geochim. Cosmochim. Acta*, *71*(12), 2936–2946, doi:10.1016/j.gca.2007.04.003.

Grossman, E. L., and T. L. Ku (1986), Oxygen and carbon fractionation in biogenic aragonite: Temperature effects, *Chem. Geol.*, *59*, 59–74, doi:10.1016/0168-9622(86)90057-6.

Habe, T. (1965), The arcid subfamily Anadarinae in Japan and its adjacent areas (Mollusca), *Bull. Natl. Sci. Mus. Tokyo*, *8*, 71–85.

Hikida, Y. (1996), Shell structure and its differentiation in the Veneridae (Bivalvia) [in Japanese with English abstract], *J. Geol. Soc. Jpn.*, *102*, 847–865, doi:10.5575/geosoc.102.847.

Irie, T., and K. Fischer (2009), Ectotherms with a calcareous exoskeleton follow the temperature-size rule—Evidence from field survey, *Mar. Ecol. Prog. Ser.*, *385*, 33–37, doi:10.3354/meps08090.

Irie, T., N. Morimoto, and K. Fischer (2013), Higher calcification costs at lower temperatures do not break the temperature-size rule in an intertidal gastropod with determinate growth, *Mar. Biol.*, *160*(10), 2619–2629, doi:10.1007/s00227-013-2256-y.

Ishimura, T., U. Tsunogai, and T. Gamo (2004), Stable carbon and oxygen isotopic determination of sub-microgram quantities of $CaCO_3$ to analyze individual foraminiferal shells, *Rapid Commun. Mass Spectrom.*, *18*, 2883–2888, doi:10.1002/rcm.1701.

Joubert, C., C. Linard, G. Le Moullac, C. Soyez, D. Saulnier, V. Teaniniuraitemoana, Ky. Chin Long, and Y. Gueguen (2014), Temperature and food influence shell growth and mantle gene expression of shell matrix proteins in the Pearl Oyster *Pinctada margaritifera*, *PloS one*, *9*(8), e103944, doi:10.1371/journal.pone.0103944.

Kennish, M. J., R. A. Lutz, and D. G. Rhoads (1980), Preparation of acetate peels and fractured sections for observation of growth patterns within the bivalve shell, in *Skeletal Growth of Aquatic Organisms: Biological Records of Environmental Change (Topics in Geobiology)*, edited by D. C. Rhoads and R. A. Lutz, pp. 597–601, Plenum, N. Y.

Kim, S. T., J. R. O'Neil, C. Hillaire-Marcel, and A. Mucci (2007), Oxygen isotope fractionation between synthetic aragonite and water: Influence of temperature and Mg^{2+} concentration, *Geochim. Cosmochim. Acta*, *71*(19), 4704–4715, doi:10.1016/j.gca.2007.04.019.

Klein, R. T., K. C. Lohmann, and C. W. Thayer (1996), Sr/Ca and $^{13}C/^{12}C$ ratios in skeletal calcite of *Mytilus trossulus*: Covariation with metabolic rate, salinity, and carbon isotopic composition of seawater, *Geochim. Cosmochim. Acta*, *60*(21), 4207–4221, doi:10.1016/S0016–7037(96)00232-3.

Kobayashi, I. (1971), Internal shell microstructure of recent Bivalvian Molluscs, *Sci. Rep. Niigata Univ., Ser. E*, *2*, 1–50.

Kobayashi, I. (1976a), Internal structure of the outer shell layer of *Anadara olluscani* (Schrenck) [in Japanese], *Venus*, *35*, 63–72.

Kobayashi, I. (1976b), The change of internal shell structure of *Anadara ninohensis* (Okuta) during the shell growth, *J. Geol. Soc. Jpn.*, *82*, 441–447.

Kobayashi, I. and H. Kamiya (1968), Microscopic observations on the shell structure of bivalves-part III genus *Anadara* [in Japanese with English abstract], *J. Geol. Soc. Jpn.*, *74*, 351–362.

Kouchinsky, A. (2000), Shell microstructures in early Cambrian molluscs, *Acta. Palaeontol. Polonica*, *45*(2), 119–150.

Lorrain, A., Y. M. Paulet, L. Chauvaud, R. Dunbar, D. Mucciarone, and M. Fontugne (2004), δ^{13}C variation in scallop shells: Increasing metabolic carbon contribution with body size?, *Geochim. Cosmochim. Acta*, *68*(17), 3509–3519, doi:10.1016/j.gca.2004.01.025.

Marie, B., C. Joubert, A. Tayalé, I. Zanella-Cléon, C. Belliard, D. Piquemal, N. Cochennec-Laureau, F. Marin, Y. Gueguen, and C. Montagnani (2012), Different secretory repertoires control the biomineralization processes of prism and nacre deposition of the pearl oyster shell, *Proc. Natl. Acad. Sci. U. S. A.*, *P109*(51), 20986–20991, doi:10.1073/pnas.1210552109.

Matsukuma, A., and T. Okutani (2000), Family Arcidae, Order Arcoida, in *Marine Mollusks in Japan*, edited by T. Okutani, pp. 844–855, Tokai Univ. Press, Tokyo.

McConnaughey, T. A. (2003), Sub-equilibrium oxygen-18 and carbon-13 levels in biological carbonates: Carbonate and kinetic models, *Coral Reefs*, *22*(4), 316–327, doi:10.1007/s00338-003-0325-2.

McConnaughey, T. A., and D. P. Gillikin (2008), Carbon isotopes in mollusk shell carbonates, *Geo-Mar. Lett.*, *28*(5-6), 287–299, doi:10.1007/s00367-008-0116-4.

Mehrbach, C., C. H. Culberson, J. E. Hawley, and R. M. Pytkowicz (1973), Measurement of the apparent dissociation constants of carbonic acid in seawater at atmospheric pressure, *Limnol. Oceanogr.*, *18*(6), 897–907.
Meyers, M. A., A. Y. M. Lin, P. Y. Chen, and J. Muyco (2008), Mechanical strength of abalone nacre: Role of the soft organic layer, *J. Mech. Behavior Biomedical Mater.*, *1*(1), 76–85, doi:10.1016/j.jmbbm.2007.03.001.
Millero, F. J. (1995), Thermodynamics of the carbon dioxide system in the oceans, *Geochim. Cosmochim. Acta*, *59*(4), 661–677, doi:10.1016/0016-7037(94)00354-O.
Minobe, F. (2007), To stabilize a cultivation method of *Scapharca broughtonii*, in *Fishery Technology Information of Aomori Prefecture, Fishery Technology Review Meeting, in Aomori Prefecture*, [in Japanese], pp. 24–28, Aomori Prefecture, Aomori.
Nakashima, R., A. Suzuki, and T. Watanabe (2004), Life history of the Pliocene scallop Fortipecten, based on oxygen and carbon isotope profiles, *Palaeogeogr. Palaeoclimatol. Palaeoecol.*, *211*(3), 299–307, doi:10.1016/j.palaeo.2004.05.011.
Nishida, K., R. Nakashima, R. Majima, and Y. Hikida (2011), Ontogenetic changes in shell microstructures in the cold seep-associated bivalve, *Conchocele bisecta* (Bivalvia: Thyasiridae), *Paleontol. Res.*, *15*, 193–212, doi:10.2517/1342-8144-15.4.193.
Nishida, K., T. Ishimura, A. Suzuki, and T. Sasaki (2012), Seasonal changes in the shell microstructure of the bloody clam, *Scapharca broughtonii* (Mollusca: Bivalvia: Arcidae), *Palaeogeogr. Palaeoclimatol. Palaeoecol.*, *363–364*, 99–108, doi:10.1016/j.palaeo.2012.08.017.
Noda, H., (1966), The Cenozoic Arcidae of Japan, *Sci. Rep. Tohoku Univ., Ser. 2*, *38*, 1–161.
Noda, H. (1986), Origin and migration of *Anadara*—Especially the genus *Hawaiarca* (Bivalvia), *Palaeontol. Soc. Jpn. Spec. Pap.*, *29*, 57–76.
O'Dea, A., and B. Okamura (2000), Intracolony variation in zooid size in cheilostome bryozoans as a new technique for investigating palaeoseasonality, *Palaeogeogr. Palaeoclimatol. Palaeoecol.*, *162*, 319–332, doi:10.1016/S0031-0182(00)00136-X.
Orr, J. C., et al. (2005), Anthropogenic ocean acidification over the twenty-first century and its impact on calcifying organisms, *Nature*, *437*(7059), 681–686, doi:10.1038/nature04095.
Owen, E. F., A. D. Wanamaker, S. C. Feindel, B. R. Schöne, and P. D. Rawson (2008), Stable carbon and oxygen isotope fractionation in bivalve (*Placopecten magellanicus*) larval aragonite, *Geochim. Cosmochim. Acta*, *72*(19), 4687–4698, doi:10.1016/j.gca.2008.06.029.
Owen, R., H. Kennedy, and C. Richardson (2002), Isotopic partitioning between scallop shell calcite and seawater: Effect of shell growth rate, *Geochim. Cosmochim. Acta*, *66*(10), 1727–1737, doi:10.1016/S0016-7037(01)00882-1.
Popp, B. N., F. A. Podosek, J. C. Brannon, T. F. Anderson, and J. Pier (1986), $^{87}Sr/^{86}$ Sr ratios in Permo-Carboniferous sea water from the analyses of well-preserved brachiopod shells, *Geochim. Cosmochim. Acta*, *50*(7), 1321–1328, doi:10.1016/0016-7037(86)90308-X.
Ragland, P. C., O. H. Pilkey, and B. W. Blackwelder (1979), Diagenetic changes in the elemental composition of unrecrystallized mollusk shells, *Chem. Geol.*, *25*(1), 123–134, doi:10.1016/0009-2541(79)90088-3.
Robbins, L. L., M. E. Hansen, J. A. Kleypas, and S. C. Meylan (2010), CO2CALC—A user-friendly seawater carbon calculator for Windows, Max OS X, and iOS (iPhone), *U.S. Geol. Surv. Open File Rep.*, 2010–1280, 17 p.
Rush, P. F., and H. S. Chafetz (1990), Fabric-retentive, non-luminescent brachiopods as indicators of original δ^{13}C and δ^{18}O composition: A test, *J. Sediment. Res.*, *60*(6), 968–981, doi:10.1306/D4267659-2B26-11D7-8648000102C1865D.
Sasaki, R. (1997), A review of larval recruitment processes of *Scapharca broughtonii* in Sendai bay (Japan), *Bull. Miyagi Prefecture Fish. Res. Dev. Cent.*, *15*, 69–79.
Sato, K., R. Nakashima, R. Majima, H. Watanabe, and T. Sasaki (2013), Shell Microstructures of Five Recent Solemyids from Japan (Mollusca: Bivalvia), *Paleontol. Res.*, *17*, 69–90, doi:10.2517/1342-8144-17.1.69.
Shimamoto, M. (1986), Shell microstructure of the Veneridae (Bivalvia) and its phylogenetic implications, *Sci. Rep. Tohoku Univ., Ser. 2*, *56*, 1–39.
Stott, L. D. (2002), The influence of diet on the δ^{13}C of shell carbon in the pulmonate snail *Helix aspersa*, *Earth Planet. Sci. Lett.*, *195*(3), 249–259. doi:10.1016/S0012-821X(01)00585-4.
Sugiura, D., S. Katayama, S. Sasa, and K. Sasaki (2014). Age and Growth of the Ark Shell *Scapharca broughtonii* (Bivalvia, Arcidae) in Japanese Waters, *J. Shellfish Res.*, *33*(1), 315–324, doi:10.2983/035.033.0130.
Taylor, J. D. (1963), The structural evolution of the bivalve shell, *Palaeontology*, *16*, 519–536.
Taylor, J. D., and M. Layman (1972), The mechanical properties of Bivalve (Mollusca) shell structures, *Palaeontology*, *15*, 73–87.
Taylor, J. D., W. J. Kennedy, and A. Hall (1969), The shell structure and mineralogy of the Bivalvia, Introduction, Nuculacea-Trigonacea, *Bull. Br. Mus. Nat. Hist. Zool.*, *22*, 1–125.
Taylor, J.D., W. J. Kennedy, and A. Hall (1973), The shell structure and mineralogy of the Bivalvia, Lucinacea-Clavagellacea, Conclusions, *Bull. Br. Mus. Nat. Hist. Zool.*, *22*, 255–295.
Ubukata, T. (2000), Theoretical morphology of composite prismatic, fibrous prismatic and foliated shell microstructures in bivalves, *Venus*, *59*(4), 297–305.
Ubukata, T. (2001a), Nucleation and growth of crystals and formation of cellular pattern of prismatic shell microstructure in bivalve molluscs, *Forma*, *16*, 141–154.
Ubukata, T. (2001b), Geometric pattern and growth rate of prismatic shell structures in Bivalvia, *Paleontol. Res.*, *5*, 33–44.
Uozumi, S., and S. Suzuki (1981), The evolution of shell structures in the Bivalvia, in *Study of Molluscan Paleobiology* [in Japanese], Professor Masae Omori memorial volume, Edited by T. Habe and M. Omori, pp. 63–77, Professor Masae Omori memorial volume Publication Committee, Niigata Univ., Niigata.
Vendrasco, M. J., S. M. Porter, A. Kouchinsky, G. Li, and C. Z. Fernandez (2010), New data on molluscs and their shell microstructures from the Middle Cambrian Gowers Formation, Australia, *Paleontology*, *53*(1) 97–135, doi:10.1111/j.1475-4983.2009.00922.x.
Watanabe, T., and T. Oba (1999), Daily reconstruction of water temperature from oxygen isotopic ratios of a modern *Tridacna* shell using a freezing microtome sampling technique, *J. Geophys. Res.*, *104*(C9), 20,667–20,674, doi:10.1029/1999JC900097.
Watanabe, T., A. Suzuki, H. Kawahata, H. Kan, and S. Ogawa (2004), A 60-year isotopic record from a mid-Holocene fossil giant clam (*Tridacna gigas*) in the Ryukyu Islands: Physiological and paleoclimatic implications, *Palaeogeogr. Palaeoclimatol. Palaeoecol.*, *212*(3), 343–354, doi:10.1016/j.palaeo.2004.07.001.
Weiss, R. F., R. A. Jahnke, and C. D. Keeling (1982), Seasonal effects of temperature and salinity on the partial pressure in seawater, *Nature*, *300*, 511–513, doi:10.1038/300511a0.
Yang, W., G. P. Zhang, X. F. Zhu, X. W. Li, and M. A. Meyers (2011), Structure and mechanical properties of *Saxidomus purpuratus* biological shells, *J. Mech. Behavior Biomedical Mater.*, *4*, 1514–1530, doi:10.1016/j.jmbbm.2011.05.021.
Yara, Y., M. Vogt, M. Fujii, H. Yamano, C. Hauri, M. Steinacher, N. Gruber, and Y. Yamanaka (2012), Ocean acidification limits temperature-induced poleward expansion of coral habitats around Japan, *Biogeosciences*, *9*(12), 4955–4968, doi:10.5194/bg-9-4955-2012.
Zhang, C., and R. Zhang (2006), Matrix proteins in the outer shells of molluscs, *Mar. Biotechnol.*, *8*(6), 572–586, doi:10.1007/s10126-005-6029-6.